EARTH'S CRYOSPHERE
SCIENTIFIC JOURNAL

Earth's Cryosphere, 2022, vol. XXVI, No. 5, pp. 3–11

PHYSICAL AND CHEMICAL PROCESSES IN FROZEN GROUND AND ICE

EXPERIMENTAL STUDIES AND A NEW MODEL OF THE WORKMAN–REYNOLDS FREEZING POTENTIAL

A.V. Shavlov[1,*], A.A. Yakovenko[2], E.S. Yakovenko[2]

[1] *Earth Cryosphere Institute, Siberian Branch of the Russian Academy of Sciences, Malygina St. 86, Tyumen, 625000 Russia*
[2] *Tyumen Industrial University, Volodarskogo St. 38, Tyumen, 625000 Russia*

**Corresponding author; e-mail: shavlov@ikz.ru*

New experimental data have been obtained on the Workman–Reynolds freezing potential of water and the electric current from an external source through the ice melting front. We propose a new model of the phenomenon that considers capturing the protons and hydroxide ions by interstitials of the ice lattice serving as charge traps. The model provides a semiquantitative explanation of the observed features of the phenomenon.

Keywords*: Workman–Reynolds freezing potential, crystallization rate, melting, proton, interstitial, electrical breakdown.*

Recommended citation: Shavlov A.V., Yakovenko A.A., Yakovenko E.S., 2022. Experimental studies and a new model of the Workman–Reynolds freezing potential. Earth's Cryosphere **26** (5), 3–11.

INTRODUCTION

The Workman–Reynolds electric freezing potential appears at the ice/water interface while freezing of pure water or diluted aqueous solutions [*Workman, Reynolds, 1950*]. This phenomenon was discovered more than a half-century ago and still arouses unrelenting interest among researchers in fundamental and applied sciences. In terms of fundamental science, it is a challenge to find out the mechanism of the freezing potential at the molecular level. The solution to this problem would strengthen the development of applied sciences searching for the connection of this phenomenon, for example, with the origin of lightning electricity [*Workman, Reynolds, 1950; Pruppacher et al., 1968; Orville, 2001*] or with the acceleration of chemical reactions while freezing of the solutions [*Sergeev, Batyuk, 1978; Moskovits, Ozin, 1979; Kazakov, Lotnik, 1987*]. In geocryology, possible relationship between the Workman–Reynolds potentials and the observed acceleration of corrosion of metal constructions and structures in contact with ice and permafrost is considered [*Hanley, 1985; Shavlov et al., 2006; Velikotskiy, 2010*]. The possibility of accelerating water migration and increasing frost heaving intensity are also associated with the Workman–Reynolds potentials [*Korkina, 1965; Yarkin, 1982*]. The latter is consistent with the experimentally established fact of frost heaving intensification within an external electric field [*Novikova, 1985*]. Thus, the interest of scientists to investigate the mechanism of freezing potential is substantiated by the importance of solving applied problems.

Let us consider the main physical characteristics of the Workman–Reynolds freezing potential. It reaches maximum values of ~10^2 V for pure water and diluted aqueous solutions with concentrations of <10^{-4} M and pH 6.8, which is close to the pH of pure water [*Kachurin et al., 1967*]. While freezing of the distilled water, the ice becomes positively charged with respect to water. Depending on the time after the crystallization start, the potential increases from zero to maximum value within ~10^2 s and then slowly decreases [*Wilson, Haymet, 2008a,b, 2010; Haymet, Wilson, 2017*]. Depending on the crystallization rate, the potential passes through its maximum at the rate of ~10^{-5} m/s [*Kachurin et al., 1967; Melnikova, 1969*]. The thickness of charged ice layer adjacent to the crystallization front is ~10^{-3} m [*Cobb, 1964; LeFebre, 1967; Mel'nikova, 1969; Rozental', Chetin, 1974*]. Almost all of the electric potential change between ice and solution is concentrated exactly within this layer. The thickness of charged layer ahead of the crystallization front in solution does not exceed several molecular layers [*Melnikova, 1969*]. The contribution of this layer to the freezing potential is insignificant. With the opposite direction of the phase transformation (ice melting), interfacial potentials are not observed [*Rozental', Chetin, 1974*].

Different models have been proposed for the physical explanation of the freezing potential origin. A popular one is the ionic model [*Chernov, Melnikova, 1971a,b*], based on the unequal capture of cations and anions of the initial solution by growing ice. In this

model, the main potential drop by about 1 V was reached in the ice phase. In the solution, the potential drop was an order of magnitude smaller. The crystallization potential weakly depended on the impurity concentration, distribution coefficients of anions and cations, and did not depend on the crystallization rate. Since the freezing potential reaches maximal values in the pure water and diluted aqueous solutions, a model based on the own charge carriers of water and ice – protons and hydroxide ions – was proposed [*Kachurin, 1970*]. Potential difference (10–10^2 V) between water and ice was created by unhindered penetration of protons into the solid phase. A model of the phenomenon on its own charge carriers was also proposed [*Rozental', Chetin, 1974*]. It was supposed that protons and hydroxide ions come from the liquid phase to the crystallization front due to Brownian motion and are irrevocably captured by ice. Since the Brownian velocity of protons is higher than that of hydroxide ions, ice acquires a positive electrical charge relative to water.

The mechanism of charge separation, which includes, in addition to protons and hydroxide ions, also own charge carriers – orientational defects – was considered in [*Shavlov, 2005*]. Recall that orientational defects are formed at energetically unfavorable orientations of water molecules with respect to one another [*Eisenberg, Kauzmann, 1969*]. A positively charged *D*-type orientational defect corresponds to an orientation when two protons are located on the line connecting two neighboring oxygen atoms, and a negatively charged *L*-type defect corresponds to a situation where there is not a single proton on the line. A one proton on the line is a no-defect state. According to the model proposed in that work, protons and hydroxide ions, as well as orientational defects, are partially rejected by the crystallization front and accumulate in the liquid phase. The accumulation process depends on the distribution coefficients and diffusion coefficients of charge carriers and leads to interfacial electrification. This model can explain the sign and magnitude of freezing potentials ~10^2 V in the pure water but cannot correctly describe the thickness of the charged layer in ice and the time it takes to reach the maximum potential after the onset of crystallization. The model gives too low values of these parameters – 10^{-5} m and 1 s, respectively, while the observed values are 10^{-3} m и 10^2 s.

Note that all of the above models are described by nonlinear electro-diffusion equations with the corresponding boundary conditions at the crystallization front, and their solutions are found by numerical methods. Although the freezing potential has been studied by many researchers, there are no convincing models to date to describe its occurrence [*Ozeki et al., 1991, 1992; Haymet, Wilson, 2017*]. Further experimental studies and new physical models are therefore required. This work aims to solve these tasks.

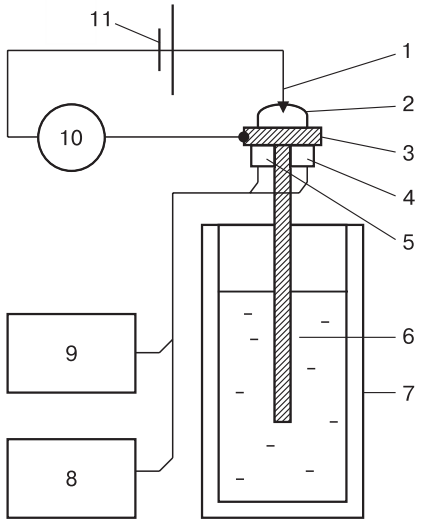

Fig. 1. Experimental setup for measuring the freezing potential of water and current from an external source through the water/ice interface.

(1) Upper electrode, (2) water drop, (3) lower electrode, (4) thermal sensor, (5) heater, (6) cold rod, (7) Dewar vessel with liquid nitrogen, (8) power supply for the heater, (9) temperature recording unit, (10) electrometer, (11) galvanic cell.

NEW EXPERIMENTAL DATA ON THE WORKMAN–REYNOLDS POTENTIAL

In this section, we present our new experimental data on the freezing potential for the pure water and data on the electrical conductivity of the water/ice interface (in the direction perpendicular to the boundary plane) while melting of ice. These data can be useful for establishing a new physical model of water freezing potential.

Authors observed the freezing potential while freezing a drop of bidistilled water using the facility shown on Fig. 1. We placed the drop of ~5 mm in diameter at the electrode 3. The electrode was in thermal contact with the upper end of the cold metal rod 6. The lower end of the metal rod was lowered into a Dewar vessel with liquid nitrogen 7. Thermal sensor 4 and electric heater 5 were fixed on the metal rod. The thermal sensor, together with the temperature recording unit 9, allowed determination of the electrode temperature with an error of ±1 K. An electric heater with power supply 8 provided heating or cooling of the electrode at a rate of ~0.5 K/s. Electrode 3, as well as the upper thin-wire electrode 1 touching the water drop, were connected to an electrometer. In the voltage measurement mode, the input resistance of the electrometer was 10^{12} Ohm (this is a typical value of the input resistance in experiments on Workman–Reynolds potentials described

in the literature). It did not significantly shunt the freezing potential of the drop. In the current measurement mode, the input resistance of the electrometer was many times less than the internal resistance of a water drop, which in our experiments was no less than $2 \cdot 10^5$ Ohm. The current in the circuit was excited by a galvanic cell 11 with a voltage of 7.5 V. In the experiments, the freezing front of the drop (or the melting front) was located approximately parallel to the electrode surface 3.

The typical temperature dependence of the freezing potential of a drop during cooling of the lower electrode at a rate of 0.5 K/s is shown on Fig. 2. The drop has been freezing during 3–5 s from the beginning of the crystallization. The difference in potentials between ice and water was also observed for 3–5 s and reached 10–20 V. Ice was positively charged. In Fig. 2, we also show the temperature dependence of the drop melting potential with the rise in temperature. It was close to zero.

Figure 3 shows the temperature dependence of current from an external source during freezing and melting of a drop. This current has nothing to do with the freezing or melting current that occurs when an external circuit is closed in the absence of an external source. The figure shows that the current from an external source flowing through the drop slowly decreases with decreasing temperature, then sharply tends to zero when the drop freezes and its electrical conductivity decreases. While heating the frozen drop, the current increases abruptly at the moment of its melting, then quickly decreases several times, tending to the initial value of the current in water. The freeze–thaw cycle with little changing result can be repeated many times.

Note that the results of the authors' experiments with freezing potentials differ slightly in magnitude and sign of the potentials from the results described in the literature and reflected in the Introduction section. New here are the data on the current from an external source through the drop during freezing and melting. These data indicate that mobile charge carriers in ice – protons, hydroxide ions, and orientational defects – are captured by traps and remain in the trapped state for a long time during freezing. Upon melting, they are released from the traps and give an increase in the current until their concentration decreases to a thermodynamically equilibrium value due to recombination. Since the electrical conductivity of pure water is controlled by protons and hydroxide ions, and orientational defects play an auxiliary role, the concentration of traps should exceed the equilibrium concentration of protons and hydroxide ions in water, which is approximately equal to 10^{20} m^{-3} [*Eisenberg, Kauzmann, 1969*]. Only in this case can a surge of current be observed in the experiment (passage of the current through a maximum) during melting. The concentration value of 10^{20} m^{-3} can easily be obtained using the pH value of pure water (6.8) by applying equation N[mol/L] = $10^{-\mathrm{pH}}$. It is important to consider the presence of such charge traps in ice in the new numerical model of the phenomenon.

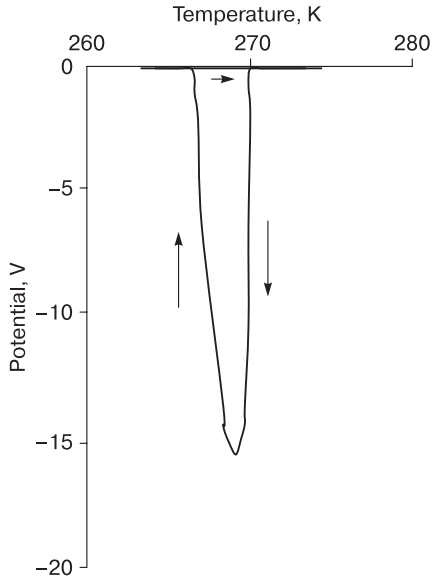

Fig. 2. Thermal dependence between the freezing potential at cooling conditions and melting potential at heating conditions of a drop.

Temperature change rate is 0.5 K/s. Arrows indicate the direction of temperature change in the experiment.

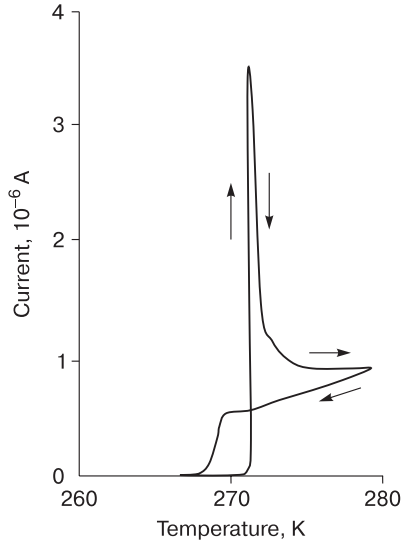

Fig. 3. Temperature dependence of the current from an external source during freezing and melting of a drop.

Temperature change rate is 0.5 K/s.

NEW MODEL OF THE WORKMAN–REYNOLDS POTENTIALS

In this study, we deal with the freezing potential of pure bidistilled water. Therefore, we do not consider ions of chemical impurities as participants in interfacial charge separation during crystallization. Obviously, ions of chemical impurities are present in water and ice in residual (uncontrolled) amounts, but their concentration is several orders of magnitude lower than the concentration of intrinsic ice lattice defects (up to 10^{-5}–10^{-4} M) capable of capturing an electric charge and participating in interfacial electrical processes. The role of such intrinsic lattice defects must be analyzed first.

Own slow-moving defects of the ice lattice – interstitials and vacancies – can claim to be charge traps in ice made from pure water. An estimate of the concentration of interstitials in ice at a temperature close to the melting point is $N_I = 10^{23}$ m^{-3} (10^{-4} M) [*Hondon et al., 1987*]. The concentration of vacancies is considered to be several orders of magnitude lower. For comparison, the concentration of mobile orientational defects in ice is $N_{D,L} = 10^{22}$ m^{-3}, the concentration of protons and hydroxide ions $N_{H,OH} = 10^{17}$ m^{-3} [*Eisenberg, Kauzmann, 1969*]. In [*Koning, Antonelli, 2008; Truffer, 2013*] concentration of interstitials $N_I = 3{\cdot}10^{22}$ m^{-3}; the concentration of vacancies $N_V = 3{\cdot}10^{17}$ m^{-3}. Thus, interstitials are the most numerous inherent slow-moving defects of the ice lattice and therefore they are more suitable for the role of charge traps in ice than other defects.

The process of accumulating the electrical charge by traps can be as follows. Let us assume that charge traps (lattice interstitials) are formed together with ice in the course of water crystallization. Then, these traps capture protons and form positively charged complexes. The possibility of the formation of such complexes was shown in [*Koning, Antonelli, 2008*]. Let us estimate the time of filling the traps with protons. In the physical sense [*Ryvkin, 1963*], the time equals $\tau_H = (v_H \sigma_H N_H)^{-1} = 0.3$ s, where $v_H = 10^3$ m/s is the thermal velocity of the proton, $\sigma_H = 3{\cdot}10^{-20}$ m^2 is the capture cross section comparable to that of a water molecule. Further, positively charged traps can capture negatively charged hydroxide ions. The trap filling time is $\tau_{OH} = (v_{OH} \sigma_{OH} N_{OH})^{-1} = 30$ s, where $v_{OH} = 10$ m/s is the thermal velocity of the hydroxide ion (it is 10^2 times less than the proton velocity, because the diffusion coefficients of these particles differ by the same factor [*Eisenberg, Kauzmann, 1969*]), $\sigma_{OH} = 3{\cdot}10^{-20}$ m^2 is the hydroxide ion capture cross section. We assume that the proton and hydroxide ion captured by the trap cannot recombine with one another. The traps can also capture charged orientational *D*- and *L*-defects, which also do not recombine with one another. The time of filling the traps with *D*- and *L*-defects is relatively short and amounts to $\tau_{D,L} = 10^{-2}$ s. It is quite probable that the traps already contain *D*- and *L*-defects by the time they are filled with protons and hydroxide ions. We assume that the traps that have captured a proton and a hydroxide ion, as well as a pair of orientational defects, become inactive with respect to subsequent captures of particles. Based on this, we conclude that ice is positively charged while its growing for the time τ_{OH} after the beginning of crystallization.

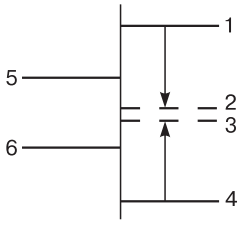

Fig. 4. Energy model of protons and hydroxide ions.

In ice: 1 and 4 are the energies of the free proton and hydroxide ion, respectively; 2 and 3 are the energies of the proton and hydroxide ion captured by the trap, respectively. In water: 5 and 6 are the energies of the free hydroxide ion and proton, respectively.

The thickness of the charged layer is $l_{OH} = v\tau_{OH}$, where v is the linear crystallization rate. Ice layers separated from the front by a distance exceeding l_{OH}, are electrically neutral. To ensure the overall electrical neutrality of the crystallizing medium, the water layer ahead of the front of crystallization must carry a negative charge. It must contain an increased amount of hydroxide ions.

Let us formulate the model of the phenomenon mathematically. The space charge of ice during crystallization is mainly formed by trapped protons and hydroxide ions, and the contribution of orientational defects is small due to small values of $\tau_{D,L}$ and the small thickness of the layer charged by them, accordingly. Therefore, we will consider protons, hydroxide ions, and traps in the model, without considering orientational defects. The energy model of protons and hydroxide ions in water and ice is explained in Fig. 4. In ice, the energy of free protons and hydroxide ions is indicated by numbers 1 and 4, respectively. They are formed in pairs due to thermal ionization of water molecules. The pair formation energy is 0.98 eV. Protons and hydroxide ions can be trapped at energy levels 2 and 3, respectively. Capture processes are indicated by arrows. Reverse thermally activated transitions from the trapped to the free state are unlikely. We will not consider them. In water, the energies of free protons and hydroxide ions are indicated by numbers 6 and 5, respectively. The energy of pair formation is ~0.5 eV. To transfer protons and hydroxide ions from water to ice, it is necessary to overcome the energy barrier. Therefore, both these and other charge carriers are largely rejected by ice during crystallization and accumulate in water.

In ice, numerous traps charged with trapped protons and hydroxide ions give the main contribution to the electrical neutrality equation. The contribution of free protons and hydroxide ions is small because of their low concentration. In addition, the volumetric charge of free protons and hydroxide ions can be concentrated near the crystallization front in a narrow layer with a thickness equal to the carrier diffusion length $(D_{\mathrm{H}}\tau_R)^{0.5} = 10^{-5}$ m, where $D_{\mathrm{H}} = 2\cdot10^{-7}$ m^2/s, $\tau_R = 7\cdot10^{-4}$ s are diffusion coefficient and proton recombination time in ice, respectively [*Eisenberg, Kauzmann, 1969*]. The thickness of the layer with charged traps is presumably 10^2 times higher. Therefore, the contribution of free protons and hydroxide ions to the volumetric charge of ice can be neglected. We assume that their concentration is equal to the equilibrium concentration $N_{\mathrm{H}} = N_{\mathrm{OH}} = 10^{17}$ m^{-3}.

Let us obtain equations and find analytical solutions for the concentrations of trapped protons p and hydroxide ions n at energy levels 2 and 3, respectively. For this, we use the continuity equation. For example, for p:

$$\frac{\partial p}{\partial t} = -\mathrm{div}\left(j_p\right) + \gamma_{\mathrm{H}} N_{\mathrm{H}}\left(S-p\right) = -\mathrm{div}\left(j_p\right) + \frac{S-p}{\tau_{\mathrm{H}}}, \quad (1)$$

where $j_p = vp$ is the flux of traps with captured protons (diffusion and electric current are absent); $\gamma_{\mathrm{H}} = v_{\mathrm{H}}\sigma_{\mathrm{H}}$ is the coefficient of proton capture by traps; S is the concentration of traps; and v is the linear crystallization rate. The second term on the right side of (1) describes the profit of protons at level 2 due to capture from level 1. This profit is proportional to the concentration of free protons N_{H} at level 1 and the concentration of empty traps $(S - p)$ at level 2. From (1) we obtain in the stationary case:

$$\frac{\partial p}{\partial t} = -v\frac{\partial p}{\partial x} + \gamma_{\mathrm{H}} N_{\mathrm{H}}\left(S-p\right) = 0,$$
$$\frac{dp}{dx} = -\frac{\gamma_{\mathrm{H}} N_{\mathrm{H}}}{v}\left(p-S\right). \quad (2)$$

The solution of Eq. (2) at a boundary condition $p\big|_{x=0} = 0$ is as follows:

$$p = S\left(1-\exp\left(-\frac{x}{l_{\mathrm{H}}}\right)\right),$$

where $l_{\mathrm{H}} = \dfrac{v}{\gamma_{\mathrm{H}} N_{\mathrm{H}}}$.

We obtain a similar solution for the concentration n of hydroxide ions captured by traps:

$$n = S\left(1-\exp\left(-\frac{x}{l_{\mathrm{OH}}}\right)\right),$$

where $l_{\mathrm{OH}} = \dfrac{v}{\gamma_{\mathrm{OH}} N_{\mathrm{OH}}}$.

Using the Poisson equation $\dfrac{dE}{dx} = \dfrac{e}{\varepsilon_I\varepsilon_0}\left(p-n\right)$, we determine the field E and the potential U in ice at boundary conditions $E\big|_{x=\infty} = 0$, $U\big|_{x=0} = 0$, where ε_I is dielectric permittivity of ice, ε_0 is electrical constant, and e is the elementary charge.

$$E = \frac{eS}{\varepsilon_I\varepsilon_0}\left(l_{\mathrm{OH}}\exp\left(-\frac{x}{l_{\mathrm{OH}}}\right) - l_H\exp\left(-\frac{x}{l_{\mathrm{H}}}\right)\right); \quad (3)$$

$$U = \frac{eS}{\varepsilon_I\varepsilon_0}\left(l_{\mathrm{OH}}^2\left(1-\exp\left(-\frac{x}{l_{\mathrm{OH}}}\right)\right) - l_{\mathrm{H}}^2\left(1-\exp\left(-\frac{x}{l_{\mathrm{H}}}\right)\right)\right). \quad (4)$$

Further, to ensure the overall electrical neutrality of the system in water, many nonequilibrium hydroxide ions are concentrated, compensating for the charge of ice. They are concentrated in the layer equal in thickness to the diffusion length. Diffusion length in water equals to $(D_{\mathrm{OH}}\tau_R)^{0.5} = 10^{-6}$ m, where $D_{\mathrm{OH}} = 7\cdot10^{-9}$ m^2/s, $\tau_R = 7\cdot10^{-5}$ s are the diffusion coefficient and recombination time of hydroxide ions, respectively [*Eisenberg, Kauzmann, 1969*].

The field strength in water near the crystallization front is equal to $E_W\big|_{x=-0} = E\big|_{x=0}\dfrac{\varepsilon_I}{\varepsilon_W}$, where ε_W is dielectric permittivity of water. The potential drop is $U_W = E_W\big|_{x=-0}\left(D_{\mathrm{OH}}\tau_R\right)^{0.5}$. For example, the potential drop will not exceed a few fractions of a Volt at the maximum value of the electric field strength in water, equal to the breakdown value $E_W = 5\cdot10^7$ V/m [*Korobeynikov, 2000*]. Thus, it should be expected that the main contribution to the freezing potential will be made by the space charge of ice, while the contribution of the space charge of water will be insignificant.

DISCUSSION

To calculate the freezing potential, we used the following values of the charge carrier's parameters in ice: concentrations of protons and hydroxide ions $N_{\mathrm{H}} = N_{\mathrm{OH}} = 10^{17}$ m^{-3}, concentration of traps $S = 10^{22}$ m^{-3}, capture coefficients $\gamma_{\mathrm{H}} = 3\cdot10^{-17}$ m^3/s, $\gamma_{\mathrm{OH}} = 3\cdot10^{-19}$ m^3/s, dielectric permittivity $\varepsilon_I = 10^4$. The value of the ice dielectric permittivity should be discussed separately. The permittivity of ice is known [*Noll, 1978*] to be depended on the frequency of the electric field (Fig. 5). The traditionally mentioned value of the permittivity $\varepsilon_I = 10^2$ is valid for the kilohertz frequency range. The phenomenon of freezing potential generation considered here lies in a different frequency range of about 10^{-1} to 10^{-2} Hz (the time for the freezing potential to reach its maximum value is tens to hundreds of seconds). In this range, the dielectric permittivity of ice is a hundred times

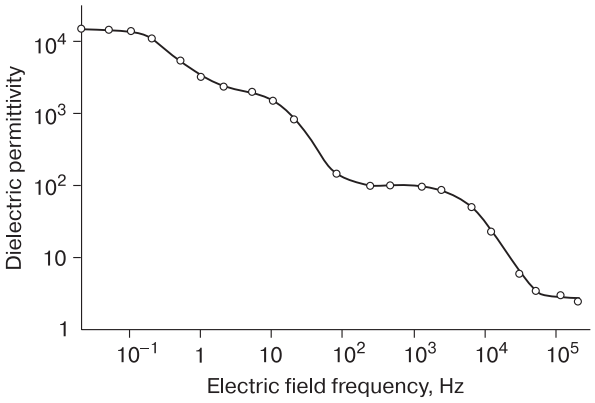

Fig. 5. Dependence between the dielectric permittivity of ice at –3 °C and the electric field frequency [*Noll, 1978*].

higher, i.e., $\varepsilon_I = 10^4$. A value close to this, $\varepsilon_I = 5 \cdot 10^4$, was obtained in the freezing potential study in the work [*Kachurin, Grigorov, 1977*]. Note that the above-discussed time of trap filling with hydroxide ions was several tens of seconds. It is quite possible that the polarization of traps (lattice interstitials) with protons, hydroxide ions, and orientational defects bound to them is responsible for the high values of the permittivity of ice at low frequencies.

Figure 6 shows the dependences of the concentration of protons captured by traps p, hydroxide ions n, and the volume charge density (p–n) in ice (in units of elementary charge) on the distance x to the crystallization front at a crystallization rate often used in experiments $v = 10^{-5}$ m/s. At low distance from the front $x < 10^{-6}$ m, traps are free of charge carriers and electrically neutral, at 10^{-6} m $< x < 10^{-3}$ m traps are filled with protons and thus positively charged, at $x > 10^{-3}$ m they are filled with protons and hydroxide ions and are electrically neutral again.

Figure 7 shows the behavior of the electric field strength E and the freezing potential U with increasing distance x from the crystallization front at crystallization rate $v = 10^{-5}$ m/s. The field strength decreases from $6 \cdot 10^6$ V/m to zero at a distance of 10^{-3} m from the front. The freezing potential increases at this distance from zero to $2 \cdot 10^3$ V and then remains unchanged as x increases.

From Figs. 6 and 7 it can be concluded that space electric charge in ice is concentrated near the phase front in a layer of ice with a thickness of 10^{-3} m (at $v = 10^{-5}$ m/s); in the same layer, the freezing potential increases to the maximum value. Further, the graph of the potential in Fig. 6 could be plotted not depending on the distance x to the front but depending on the time $t = x/v$ from the beginning of crystallization. Then, we would see that the freezing potential reaches its maximum value in 10^2 s after the onset of crystallization. We obtain that the thickness of the charged ice layer is 10^{-3} m, the time for the potential to reach its maximum value of 10^2 s, and the large potential value of 10^3 V are in satisfactory agreement with the experiments described in the Introduction.

We note that the field strength in ice near the crystallization front is $6 \cdot 10^6$ V/m. From this value, it is easy to calculate the field strength in water near the phase front. It will be $\varepsilon_I/\varepsilon_W = 10^2$ times higher than in ice, that is $6 \cdot 10^8$ V/m. This value is an order of magnitude higher than the breakdown value of the field strength in water equal to $5 \cdot 10^7$ V/m. Thus, electrical breakdown can take place in water near the crystallization front. This conclusion can explain why the crystallization front is a source of pulsed electromagnetic radiation, as well as acoustic radiation, as it was found in experiments described in [*Kachurin et al.,*

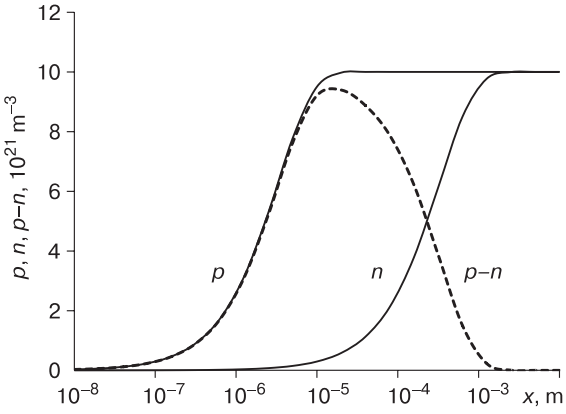

Fig. 6. Concentration of protons (p) and hydroxide-ions (n) captured by traps, and the density of space charge (p–n) in ice depending on the distance (x) to the crystallization front at crystallization rate $v = 10^{-5}$ m/s.

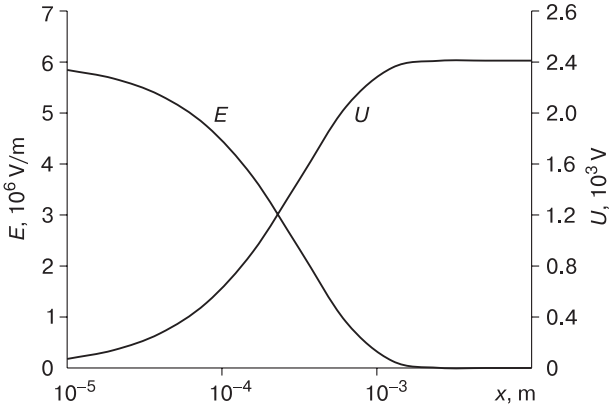

Fig. 7. Dependence of electrical field (E) and freezing potential (U) on the distance (x) to the crystallization front at crystallization rate $v = 10^{-5}$ m/s.

1982; Shibkov et al., 2002]. Electromagnetic radiation of the megahertz range was observed in the form of packets of oscillations (as in pulsed discharges) with the frequency of packets rapidly increasing with an increase in the freezing potential (up to 10 packets per second at a freezing potential of 10^2 V). Note that the authors of the cited papers have also associated electromagnetic and acoustic radiation with electric discharges in ice between crack edges due to ice cracking, but not in water. The weak point in this hypothesis seems to be precisely ice cracking, since this process requires orders of magnitude higher freezing rates [*Trokhan et al., 1984*] than in experiments on the study of Workman–Reynolds potentials.

For electrical breakdown in water, the following concepts are currently developed, such as described in [*Korobeynikov, 2000*]. Ionization processes (partial discharges according to the Paschen's Law) arise on air bubbles that previously existed in the water under the action of a breakdown electric field. After the discharge, the field in the bubble decreases due to screening of the external field by the charges deposited on the bubble walls. This causes weakening or termination of ionization processes in the bubble. The action of the field on the settled charge leads to the motion of the bubble wall and the elongation of the bubble along the field. As a result, the voltage in the bubble increases, which leads to a repeated partial discharge and the movement of a new wave of charges. This model of electrical breakdown in a liquid makes it possible to semiquantitatively explain almost all experimental dependences of the breakdown strength: on pressure, temperature, viscosity, and on the duration of the acting electrical pulse.

Fluctuations in the size of gas bubbles in a liquid during electrical breakdown, apparently, are the cause of the acoustic emission that accompanies the occurrence of freezing potentials. Density fluctuations in a thin water layer near the crystallization front were confirmed experimentally [*Bilgram et al., 1978; Bilgram, 1982*]. According to these papers, the intensity of the light scattered by the crystallization front increases sharply relative to the background value, when the crystallization rate exceeds 10^{-6} m/s. Further, a sharp increase is replaced by a more gradual increase in the intensity of scattered light with further growth of the rate of crystallization (Fig. 8). As the crystallization rate decreases from the maximum value in the experiment to zero, the scattering intensity decreases monotonously to the background value. Apparently, the electric field strength in water reaches a threshold value at a crystallization rate of 10^{-6} m/s and electrical breakdown occurs for the first time.

If we check the value of the field from Eq. (3) at crystallization rate of 10^{-6} m/s, we obtain the field strength in ice $6{\cdot}10^5$ V/m. Then, the field strength in water will be 10^2 times higher $6{\cdot}10^7$ V/m – the breakdown value of the electric field strength for water. This estimate is quite good. Here the question arises: why the intensity of light scattering does not decrease abruptly to the background value, but decreases monotonously as the crystallization rate decreases? Apparently, this happens because the electric strength of water decreases as the time of water exposure to electric discharges increases [*Korobeynikov, 2000*].

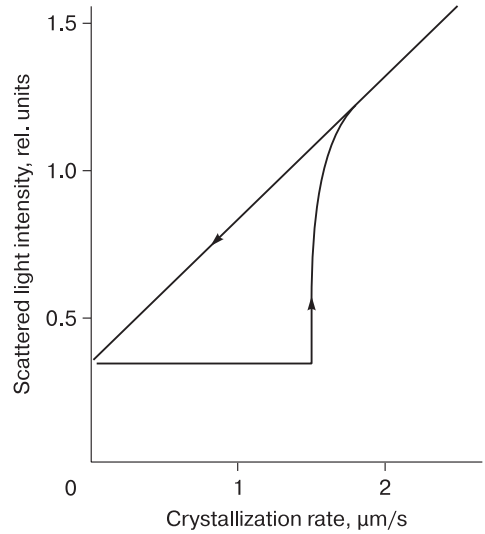

Fig. 8. Dependence between the intensity of light scattered by crystallization front and the crystallization rate [*Bilgram et al., 1978*].

Let us consider another issue formulated in the paper [*Haymet, Wilson, 2017*]. Why the freezing potential does not remain unchanged over time having reached its maximum after the onset of crystallization, but begins to slowly decrease, while the crystallization rate remains approximately constant? The time for half-reducing the potential is 15–20 min. The decrease in the crystallization potential with time can also be explained (within the framework of the model proposed here) using the idea of the existence of an electrical breakdown of water ahead of the crystallization front. During the breakdown of water, dissociation products corresponding to the phenomenon – ionized water molecules and electrons that are transformed into a hydrated state – are formed. They accumulate ahead of the front over time. They can partially be captured by the growing ice; another part is rejected by the front. Electrons are smaller and more easily embedded into the solid phase. In ice, electrons can form complexes with free protons, lowering their equilibrium concentration. Due to the ionic equilibrium ($N_H N_{OH}$ = const), the concentration of free hydroxide ions will increase (shift of the chemical equilibrium towards the alkaline side), and,

as a result, the freezing potential will decrease. This can be shown using Eq. (4). According to this equation, the potential aside from the front is equal to

$$U = \frac{eS}{\varepsilon_I \varepsilon_0} \frac{v^2}{\gamma_{OH}^2 N_{OH}^2}.$$

To decrease the freezing potential by half, the concentration of free hydroxide ions N_{OH} should increase by 1.4 times. The dependence of the freezing potential on the crystallization rate with a maximum at the rate of 10^{-5} m/s can also be explained by the accumulation of electrical breakdown products of water and the shift of chemical equilibrium in ice to the alkaline side, which is more pronounced at rates of more than 10^{-5} m/s. For the formation of a maximum, it is necessary that the concentration of N_{OH} hydroxide ions grows slightly faster at $v > 10^{-5}$ m/s than the crystallization rate v.

Note that in the proposed model the authors do not consider the presence of ions of chemical impurities. This is permissible, if their concentration is much less than the concentration of intrinsic defects – interstitials with a concentration of 10^{-5}–10^{-4} M. At a high concentration of ions of chemical impurities, their contribution to interfacial electrical processes can no longer be neglected, and the model must be developed further.

CONCLUSIONS

We briefly summarize the results achieved in this work.

We have obtained a new experimental data on the Workman–Reynolds freezing potentials and the electric current through the water-ice interface in distilled water.

We propose a new freezing potential model based on charge accumulation by traps in ice, which can be represented by interstitials – intrinsic defects of the ice lattice. The proposed model can partially quantitatively and qualitatively describe most of the features of the phenomenon listed in the Introduction section. The model can also explain the new experimental data on the increase in electric current during ice melting. This is related to ceasing of the trapping of electric charges by the interstitials and ice turning into ordinary water molecules while melting. In this case, released are protons, hydroxide ions, and orientational defects associated with them are released. During the relaxation time, they all contribute to the increase in electrical conductivity up to values exceeding equilibrium ones.

The model of the Workman–Reynolds phenomenon considered by the authors can initiate further experimental studies of electrical processes during freezing of water. It can also serve as a further development of applied research, i.e., to advance understanding of the mechanisms of chemical reactions' acceleration at the crystallization front of solutions. This is important for improving the technologies of non-destructive storage of food, biological objects, and drugs in a frozen state. The model can also be useful for understanding the mechanism and improving the technology of reducing the rate of metal structure corrosion in contact with ice.

References

Bilgram J.H., 1982. Die Dynamik des Gefrierens. *Naturwissenschaften* **69**, 472–478 (in German).

Bilgram J.H., Guttinger H., Kanzig W., 1978. Fluctuations of the ice-water interface during solidification. *Phys Rev. Lett.* **40** (21), 1394–1397.

Chernov A.A., Melnikova A.M., 1971a. Theory of electrical phenomena accompanying crystallization. I. Electric field in a crystallizing water solution of electrolyte. *Crystallografiya* **16**, 477–487 (in Russian).

Chernov A.A., Melnikova A.M., 1971b. Theory of electrical phenomena accompanying crystallization. II. Potential difference between phases during crystallization of ice and naphthalene. *Crystallografiya* **16**, 488–491 (in Russian).

Cobb A.W., 1964. *Interfacial Electrical Effects Observed during the Freezing of Water. Unpublished Report*. New Mexico Institute of Mining and Technology, Socorro, New Mexico.

Eisenberg D., Kauzmann W., 1969. *The Structure and Properties of Water*. New York, Oxford Univ. Press, 280 pp.

Hanley T.O.D., 1985. Electrical freezing potentials and corrosion rates in clay sludge. *Can. Geotech.* **22**, 599–604.

Haymet A.D.J., Wilson P.W., 2017. TheWorkman–Reynolds "Freezing Potential": A new look at the inherent physical process. *J. Molecular Liquids* **228**, 243–246.

Hondon T., Azuma K., Higashi A., 1987. Self-interstitials in ice. *J. de Physique* **48** (3), 183–187.

Kachurin L.G., 1970. Electrokinetic phenomena arising during the crystallization of liquids. *Electrokhimiya* **6** (9), 1294–1299 (in Russian).

Kachurin L.G., Bekryayev V.I., Psalomshchikov V.F., 1967. Experimental study of the electrokinetic phenomenon arising during the crystallization of aqueous solutions. *Dokl. Akad. Nauk SSSR* (Moscow) **174** (5), 1122–1130 (in Russian).

Kachurin L.G., Grigorov N.O., 1977. Electro-crystallization potentials and permittivity of aqueous solutions. *Zh. Fizich. Khimii* **51** (11), 2864–2868 (in Russian).

Kachurin L.G., Kolev S., Psalomshchikov V.F., 1982. Pulsed radio emission arising from the crystallization of water and some dielectrics. *Dokl. Akad. Nauk SSSR* (Moscow), **267**, 347–350 (in Russian).

Kazakov V.P., Lotnik S.V., 1987. *Low-Temperature Chemiluminescence*. Moscow, Nauka, 176 pp. (in Russian).

Koning M., Antonelli A., 2008. Modeling equilibrium concentrations of Bjerrum and molecular point defects and their complexes in ice. *J. Chem. Phys.* **128**, 164502.

Korkina R.I., 1965. Electric potentials in freezing solutions and their influence on migration. In: *Processes of Heat and Mass Transfer in Frozen Rocks*. Moscow, Izd. Akad. Nauk SSSR, pp. 35–39 (in Russian).

Korobeynikov S.M., 2000. *Dielectric materials. Textbook*. Novosibirsk, Izd. Novosibirsk Gos. Univ., 66 pp. (in Russian).

LeFebre V., 1967. The freezing potential effect. *J. Colloid Interface Sci.* **25** (2), 263.

Mel'nikova A.M., 1969. Separation of charges during crystallization. *Kristallografiya* **14** (3), 548–563 (in Russian).

Moskovits M., Ozin G., 1979. *Cryochemistry*. Moscow, Mir, 594 pp. (in Russian).

Noll G., 1978. The influence of the rate of deformation on the electrical properties of ice monocrystals. *J. Glaciol*. **21** (85), 277–289.

Novikova E.V., 1985. On the method of studying the effect of an electric field on cryogenic migration in finely dispersed soils. In: *Methods for Studying Seasonally Freezing and Frozen Soils*. Moscow, Stroyizdat, pp. 9–13 (in Russian).

Orville R., 2001. *Glossary of Meteorology*. – http://www.met.tamu.edu/personnel/faculty/orville/Glossary.htm (13 Mar. 2001).

Ozeki S., Sashida N., Kakei K., Suzuki T., Kaneko K., 1991. Fine-structure of freezing potential of aqueous lithium-chloride solutions and its oscillation due to trace ethanol. *Langmuir* **7**, 821–823.

Ozeki S., Sashida N., Samata T., Kaneko K., 1992. Oscillation of the freezing potential of aqueous lithium-chloride solutions containing ethanol. *J. Chem. Soc. Faraday Trans.* **88**, 2511–2516.

Pruppacher H.R., Steinberger E.H., Wang T.L., 1968. On the electrical effects that accompany the spontaneous growth of ice in supercooled aqueous solutions. *J. Geophys. Res.* **73**, 571–584.

Rozental' O.M., Chetin F.Ye., 1974. *Multilayer Structural Ordering in Heterogeneous Processes of Ice Formation*. Sverdlovsk, Izd. Gos. Pedag. Inst., 134 pp. (in Russian).

Ryvkin S.M., 1963. *Photoelectric Phenomena in Semiconductors*. Moscow, Fizmatlit, 494 pp. (in Russian).

Sergeev G.B., Batyuk V.A., 1978. *Cryochemistry*. Moscow, Khimiya, 296 pp. (in Russian).

Shavlov A.V., 2005. Electric potential of crystallization of water and solutions. The role of protons and orientation defects. *Zh. Fizich. Khimii* **79** (8), 1626–1630 (in Russian).

Shavlov A.V., Pisarev A.D., Ryabtseva A.A., 2006. Dynamics of electrical conductivity of metal films in ice during its structural transformation. Recombination-proton mechanism of corrosion acceleration. *Kriosfera Zemli* **10** (3), 42–48 (in Russian).

Shibkov A.A., Golovin Yu.I., Zheltov M.A., Korolev A.A., Leonov A.A., 2002. In situ monitoring of growth of ice from supercooled water by a new electromagnetic method. *J. Crystal Growth* **236**, 434–440.

Trokhan A.M., Lapshin A.I., Gudzenko O.I., 1984. Cryoluminescence of liquids. *Dokl. Akad. Nauk SSSR* **275** (1), 83–86 (in Russian).

Truffer M., 2013. *Ice Physics*. Fairbanks, USA, University of Alaska, 120 pp.

Velikotskiy M.A., 2010. Corrosion activity of soils in various natural zones. *Byull. Mosk. Gos. Univ. Ser. 5. Geogr.*, no. 1, 21–27 (in Russian).

Wilson P.W., Haymet A.D.J., 2008a. Workman–Reynolds freezing potential measurements between ice and dilute salt solutions for single ice crystal faces. *J. Phys. Chem.* **112** (37), 15260–15261.

Wilson P.W., Haymet A.D.J., 2008b. New measurements of the Workman Reynolds Freezing Potential between ice and dilute salt solutions for single ice crystal faces. *J. Phys. Chem. B*. **112** (37), 11750–11755.

Wilson P.W., Haymet A.D.J., 2010. The effect of ice growth rate on the measured Workman-Reynolds freezing potential between ice and dilute NaCl solutions. *J. Phys. Chem. B*. **114** (39), 12585–12588.

Workman E.J., Reynolds S.E., 1950. Electrical phenomena occurring during freezing of dilute aqueous solutions, and their possible relationship to thunderstorm activity. *Phys. Rev.* **78**, 254–259.

Yarkin I.G., 1982. Soil polarization during freezing and its relationship with water migration and frost heaving. In: *Proc. Research Institute of Foundations and Underground Structures*. Issue. 75. Moscow, Stroyizdat, pp. 53–59 (in Russian).

Received August 3, 2021
Revised June 26, 2022
Accepted September 20, 2022

Translated by Yu.A. Dvornikov